



# Simultaneous SERS-decoding detection of multiple pathogens in drinking water with home-made portable double-layer filtration and concentration device

Huqi Wu<sup>1</sup> · Yan Gao<sup>1</sup> · Qi Chen<sup>1</sup> · Li Yao<sup>4</sup> · Bangben Yao<sup>1,2</sup> · Jielin Yang<sup>3</sup> · Wei Chen<sup>1</sup>

Received: 6 April 2024 / Accepted: 5 June 2024 / Published online: 28 June 2024  
© The Author(s), under exclusive licence to Springer-Verlag GmbH Austria, part of Springer Nature 2024

## Abstract

The engineering of a home-made portable double-layer filtration and concentration device with the common syringe for rapid analysis of water samples is reported. The core elements of the device were two installed filtration membranes with different pore sizes for respective functions. The upper filtration membrane was used for preliminary intercepting large interfering impurities (*interception membrane*), while the lower filtration membrane was used for collecting multiple target pathogens (*enrichment membrane*) for determination. This combination can make the contaminated environmental water, exemplified by surface water, filtrated quickly through the device and just retained the target bacteria of *Escherichia coli* O157:H7, *Staphylococcus aureus*, and *Listeria monocytogenes* on the lower enrichment membrane. Integrating with surface-enhanced Raman spectra (SERS) platform to decode the SERS-Tags (SERS-Tag<sup>CVa</sup>, SERS-Tag<sup>R6G</sup>, and SERS-Tag<sup>MB</sup>) already labeled on each of the enriched bacteria based the antibody-mediated immuno-recognition effect, fast separation, concentration, and detection of multiple pathogenic bacteria from the bulk of contaminated environmental water were realized. Results show that within 30 min, all target bacteria in the lake water can be simultaneously and accurately measured in the range from 10<sup>1</sup> to 10<sup>6</sup> CFU mL<sup>-1</sup> with detection limit of 10.0 CFU mL<sup>-1</sup> without any pre-culture procedures. This work highlights the simplicity, rapidness, cheapness, selectivity, and the robustness of the constructed method for simultaneous detecting multiple pathogens in aqueous samples. This protocol opens a new avenue for facilitating the development of versatile analytical tools for drinking water and food safety monitoring in underdeveloped or developing countries.

**Keywords** Filtration device · SERS · Waterborne pathogen · Multiple detection · Signal decoding

## Introduction

Pathogenic bacteria are considered to be serious threat to human health in developed, developing, and underdeveloped countries worldwide [1, 2]. Awareness is growing that aqueous environment, especially water, is susceptible to be contaminated by various bacteria and induces the outbreak of waterborne disease [3]. Evidences have shown that bacteria such as *Escherichia coli* O157:H7 (*E. coli* O157:H7), *Staphylococcus aureus* (*S. aureus*), *Listeria monocytogenes* (*L. monocytogenes*), and *Pseudomonas aeruginosa* [4–7] have been found in groundwater, surface water, and domestic sewage [8–10]. These harmful waterborne pathogens cause life-threatening infectious diseases including hemorrhagic colitis, hemolytic uremic syndrome, septicopyemia, and septicemia [11–13] via directly drinking of contaminated water or indirectly consumption of contaminated fruits and vegetables irrigated by contaminated water. A consensus has been

✉ Wei Chen  
chenweishnu@163.com

Jielin Yang  
yangjielin@customs.gov.cn

- <sup>1</sup> Engineering Research Center of Bio-process, MOE, School of Food and Biological Engineering, Intelligent Manufacturing Institute, Hefei University of Technology, Hefei 230009, P. R. China
- <sup>2</sup> Anhui Province Institute of Product Quality Supervision & Inspection, Hefei 230051, P.R. China
- <sup>3</sup> Technical Centre for Animal, Plant and Food Inspection and Quarantine of Shanghai Customs, Shanghai 200135, China
- <sup>4</sup> School of Food Science and Bioengineering, Changsha University of Science and Technology, Changsha, China

reached that control of waterborne diseases can be greatly improved if bacterial infections could be timely detected and identified [14, 15]. As a result, developing of rapid and accurate detection methods with low cost and simplicity for simultaneous detecting multiple pathogenic bacteria in water is of great significance to reduce or avoid the potential risk of human infection or losing lives.

Generally, the most matured techniques for pathogenic bacteria detection are conventional culture- and molecular amplification-based methods [16, 17]. Although the applications of these methods have achieved impressive progresses for pathogens identification and analysis, the culture methods generally need lengthy culture at least 24 h to several days to obtain the final conclusive results, which lead to undesirable delays in completion of the analysis and life safety threat. Besides, the identification of pathogens is usually single target analysis with the specific culture medium, and different pathogens should be cultured independently. Molecular amplification methods including polymerase chain reaction [18] (PCR), real-time PCR [19] (RT-PCR), loop-mediated isothermal amplification [20–22] (LAMP), and recombinase polymerase amplification [23] (RPA) that can amplify specific regions of nucleic acids are still facing performance-limited issues such as false-positive amplification and cross contamination especially when facing with multiple pathogens. Besides, the most representative PCR and RT-PCR also require skilled technicians for careful handling of the specialized instruments and a certain level of expertise for the interpretation of final results, inhibiting the popularization of molecular methods. Immune principle-based methods have also been adopted for bacteria determination. Previous reported methods based on immunorecognitions [24, 25] needs complex interface construction and multistep immobilization, recognition, and washing. They are not user-friendly in terms of operation simplicity, sensitivity, and efficiency. Additionally, it is widely recognized that water samples are usually contaminated with different pathogenic bacteria. Current researches mainly focus on detecting only one kind of target bacteria, which cannot meet the demand of accurate estimating pathogen categories and concentrations in water [26, 27]. In this respect, design of new analytical strategies for overcoming abovementioned limitations and simultaneous monitoring multiple target pathogens is vital to acquire the evaluation information of water quality. Fortunately, surface-enhanced Raman scattering (SERS) is an ultrasensitive and noninvasive molecular spectroscopy technique [28–30]. With well-recognized characteristics of high sensitivity, high photostability and detection efficiency, low environmental interference, and less reagent consumption, SERS-assisted biosensors are ideal candidates for pathogenic bacteria detections [31–33]. More importantly, the narrow bands/fingerprint of Raman molecules offers SERS biosensing strategies a powerful multiplex screening capability and therefore is very suitable for simultaneous analyzing multiple analytes.

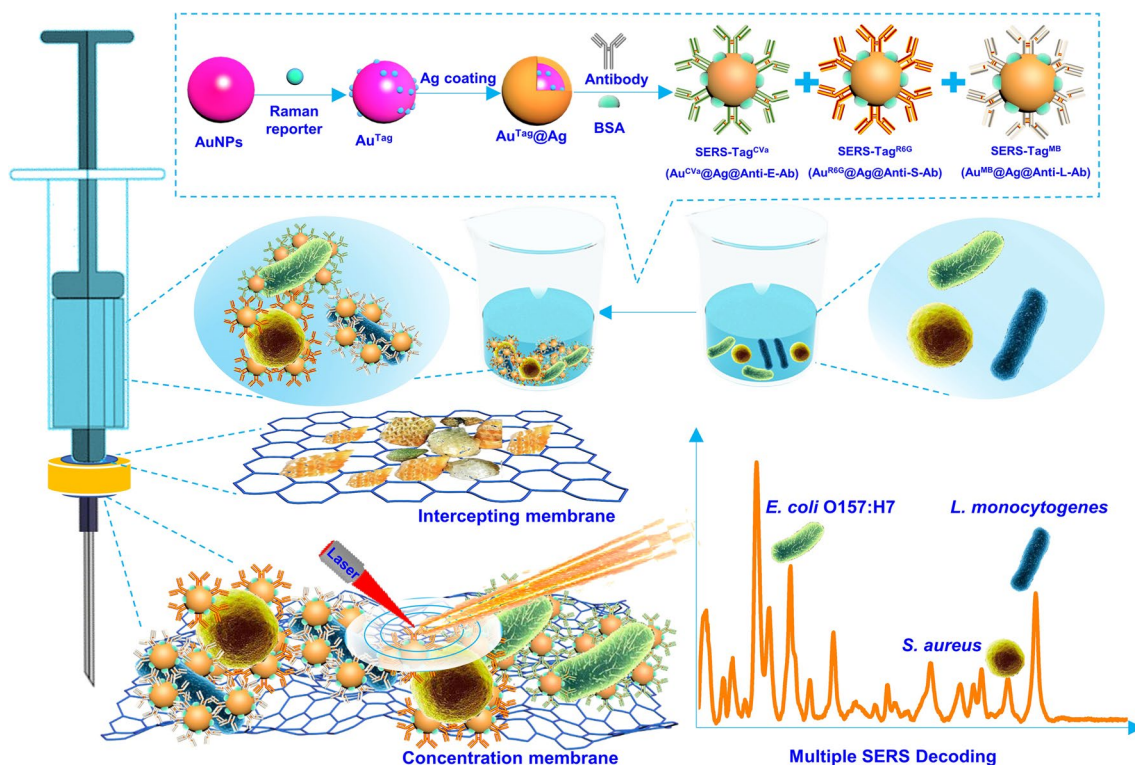
In 2015, a piece of breaking news about *The drinkable book* has greatly aroused the interest of public [34]. The book invented by “Theresa Dankovich” is actually a filtration kit equipped with a filter box and a book with pages that offer both sanitation advice and function as filter sheets. The waterborne pathogenic bacteria can be attached and adsorbed onto each utilized book sheet, while the water can be filtrated through the paper page, leaving it safe for drink. Inspired by the idea of *drinkable book* and taken above into consideration, in this study, we have concisely engineered a portable double-layer filtration device for bacteria detection and water quality control. The two layered filtration membrane can take effect to remove the interferants and retain the target pathogens for analysis. Different SERS-Tags as Raman signal reporting units were adopted and incubated with water samples for fast recognition, separation, concentration, and identification of multiple waterborne pathogens including *E. coli* O157:H7, *S. aureus*, and *L. monocytogenes* in lake water with this designed two-membrane device. Each of the SERS-Tag (antibody-conjugated Au<sup>Tag</sup>@Ag) consists of an Au@Ag nanoparticle as Raman enhanced substrate, an adsorbed Raman reporter dye (CVa, R6G, and MB) to produce characteristic SERS signal, and a specific antibody to recognize and bind with target pathogen.

Structurally, this two-membrane filtration device is a remolded syringe with an upper layer filtration membrane with pore size of 30  $\mu\text{m}$  (*intercepting membrane*) and a lower layer filtration membrane with pore size of 220 nm (*enrichment membrane*). When utilized for multiple SERS decoding assay, as shown in Scheme 1, the mixed SERS-Tags (SERS-Tag<sup>CVa</sup>, SERS-Tag<sup>R6G</sup>, and SERS-Tag<sup>MB</sup>) would firstly be incubated with water samples to bind to their respective target pathogenic bacteria (*E. coli* O157:H7, *S. aureus*, and *L. monocytogenes*) via the specific immune recognition. This incubated water sample was made to flow through the double-layer filtration device quickly. During this process, objects with large size including sand, plankton etc. are entrapped by the upper intercepting membrane (pore size of 30  $\mu\text{m}$ ), while three target pathogens can be intercepted and concentrated by the lower enrichment membrane (pore size of 220 nm). Simultaneous and direct SERS measurement of multiple target pathogens is realized on the enrichment membrane. This two-membrane device holds great potential for water quality control in resource-limited settings.

## Materials and methods

### Materials and instruments

Chloroauric acid, L-ascorbic acid, trisodium citrate dihydrate, silver nitrate ( $\text{AgNO}_3$ ), bovine serum albumin (BSA),



**Scheme 1** Schematic illustration of the portable double-layer filtration device with SERS-Tags as Raman signal reporting units for detecting multiple bacteria in water samples

rhodamine 6G (R6G), agarose, dNTP, DNA marker, and Taq DNA polymerase were obtained from Sangon Biotech (Shanghai, [www.sangon.com/](http://www.sangon.com/)) Co., Ltd. Methylene blue (MB) and cresyl violet acetate (CVa) were purchased from Aladdin (Shanghai, China, [www.aladdin-e.com/](http://www.aladdin-e.com/)). Anti-*E. coli* O157:H7 antibody (Anti-E-Ab), Anti-*S. aureus* antibody (Anti-S-Ab), and Anti-*L. monocytogenes* antibody (Anti-L-Ab) were purchased from Abcam (Beijing, China, [www.abcam.cn](http://www.abcam.cn)). Portable SEED3000 Raman spectrometer was provided by OCEANHOOD (OCEANHOOD, Shanghai, China) and adopted for on-site Raman measurements with a 785-nm (100 mW) laser and an acquisition time of 10 s.

### Bacterial strains

All bacterial strains including *E. coli* O157:H7, *S. aureus*, *L. monocytogenes*, *Cronobacter sakazakii* (*C. sakazakii*), *Escherichia coli* (*E. coli*), *Pseudomonas aeruginosa* (*P. aeruginosa*), and *Salmonella enteritidis* (*S. enteritidis*) were from American Type Culture Collection (ATCC) and China Microbiological Culture Collection (CMCC). See details in Table S1. They were cultured overnight in Luria–Bertani broth (Sangon Biotech Co., Ltd., Shanghai, China) at 37 °C and counted by the standard flat colony counting method [35].

### Preparation of gold nanoparticles

Preparation of AuNPs was conducted according to previously reported method with minor modification [36]. Briefly, 750  $\mu\text{L}$  of 5 g  $\text{L}^{-1}$  chloroauric acid was added to 50 mL of deionized water under vigorous stirring. After being heated to boiling, 800  $\mu\text{L}$  of 1% trisodium citrate was added immediately. Then, the solution was kept in boiling for additional 15 min and then cooled to room temperature.

### Preparation of various Au<sup>Tag</sup> for multiple bacteria

To prepare Au<sup>Tag</sup> (Au<sup>CVa</sup>, Au<sup>R6G</sup>, and Au<sup>MB</sup>), a certain amount of Raman signal molecule (10  $\mu\text{L}$  100  $\mu\text{M}$  CVa for Au<sup>CVa</sup>, 10  $\mu\text{L}$  100  $\mu\text{M}$  R6G for Au<sup>R6G</sup>, and 50  $\mu\text{L}$  10  $\mu\text{M}$  MB for Au<sup>MB</sup>) was mixed with 1 mL AuNPs. The mixture was shaken for 10 min at room temperature to make Tag molecules fully bind with AuNPs. Obtained Au<sup>Tag</sup> was purified by centrifugation at 8000 g and resuspended in 1 mL sterile water.

### Preparation of Au<sup>Tag</sup>@Ag

The preparation of Au<sup>Tag</sup>@Ag (Au<sup>CVa</sup>@Ag, Au<sup>R6G</sup>@Ag, and Au<sup>MB</sup>@Ag) was performed based on the reducing of AgNO<sub>3</sub> on the surface of Au<sup>Tag</sup> [37, 38]. In brief, 100  $\mu\text{L}$  ascorbic

acid was added into 1 mL Au<sup>Tag</sup> and stirred for 10 min. This was followed by quick adding 300  $\mu$ L 1% AgNO<sub>3</sub> under ultrasonic condition. Of note, the ultrasonic condition was maintained until the solution color changed from purple-red to orange-yellow. The final Au<sup>Tag</sup>@Ag solution was centrifuged at 10,000 g and resuspended in 1 mL sterile water.

### Preparation of SERS-Tag

To synthesize SERS-Tags (SERS-Tag<sup>CVa</sup>, SERS-Tag<sup>R6G</sup>, and SERS-Tag<sup>MB</sup>), namely, anti-*E. coli* O157:H7 antibody-conjugated Au<sup>CVa</sup>@Ag (Au<sup>CVa</sup>@Ag@Anti-E-Ab), anti-*S. aureus* antibody-conjugated Au<sup>R6G</sup>@Ag (Au<sup>R6G</sup>@Ag@Anti-S-Ab), and anti-*L. monocytogenes* antibody-conjugated Au<sup>MB</sup>@Ag (Au<sup>MB</sup>@Ag@Anti-L-Ab), the pH of Au<sup>CVa</sup>@Ag, Au<sup>R6G</sup>@Ag, or Au<sup>MB</sup>@Ag was firstly adjusted to  $\sim$ 8.0 by K<sub>2</sub>CO<sub>3</sub>. Thereafter, 4  $\mu$ L of 1 mg mL<sup>-1</sup> anti-*E. coli* O157:H7 antibody, anti-*S. aureus* antibody, or anti-*L. monocytogenes* antibody was mixed with 1 mL Au<sup>CVa</sup>@Ag, Au<sup>R6G</sup>@Ag, or Au<sup>MB</sup>@Ag, respectively. After reacting for 1 h at room temperature, the nano-conjugates were further blocked with 20  $\mu$ L 10% BSA for an additional 1 h and centrifuged at 10,000 g for 10 min to remove free antibodies and BSA. The final products were re-suspended in 1 mL stock solution (10 mM PBS) for subsequent utilization. The mixture of different SERS-Tags was added into the water samples and incubated for 10 min, and the incubated water samples were quickly treated with the constructed double-layer filtration device.

### Fabrication of the double-layer filtration device

The framework of the device composed with a syringe, a hollow polystyrene filtration tube, and two cellulose membranes with different pore sizes (30  $\mu$ m and 220 nm). The adoption of the pore size of different membranes was based on the consideration of practical application conditions and existing commercial filtration membrane. Filtration membrane with pore size of 30  $\mu$ m can guarantee the interception of most macro particles while the lower filtration membrane with pore size of 220 nm can retain most of the bacteria on the membrane. To fabricate the device, both two cellulose membranes were cut into disc shape with the diameter of 15 mm to cover the water inlet (diameter of 6 mm) and outlet (diameter of 4 mm). The hollow polystyrene tube was mechanically installed between the syringe and the needle.

### SERS decoding measurement

To perform the SERS measurement, 20  $\mu$ L of SERS-Tag<sup>CVa</sup>, 20  $\mu$ L of SERS-Tag<sup>R6G</sup>, and 20  $\mu$ L of SERS-Tag<sup>MB</sup>

were added to 10 mL of multiple bacteria-contaminated lake water samples with known bacteria concentrations and incubated for just 10 min. Then, the mixture was transferred to the constructed filtration device. To maximally avoid the non-specific absorption and removal impurities, the above operation was repeated and filtrated for 3 times. The second filtration membrane (enrichment membrane) with pore size of 220 nm was taken down and placed onto a glass slide for the collection of Raman signals. For the collection of Raman signals on the membrane, at least 10 different spots on the membrane should be performed to get the average values. Then, for the detection of each concentration, three parallel tests were conducted to obtain the average value, which was adopted for the construction of calibration plot for quantitative analysis. It is worth pointing out that the adopted water samples have all been pre-validated by both the culture method and PCR to ensure the existence of the target bacteria or not.

### Bacterial DNA extraction and PCR amplification

The extraction of bacterial DNA and PCR amplification were conducted based on the reported method [17, 39]. For DNA extraction, the lower enrichment membrane with intercepted and concentrated bacteria was immersed in 700  $\mu$ L of lysate solution (10 mM Tris-HCl, 200 mM NaCl, 5 mM EDTA, 1% SDS, pH 8.0). After adding with 30  $\mu$ L 20 mg mL<sup>-1</sup> Proteinase K and incubated at 60  $^{\circ}$ C for 10 min, the mixture was further added with 100  $\mu$ g carboxylated MNPs and kept at room temperature for 5 min. The MNPs absorbed with extracted genomic DNA were collected by magnetic separation. Finally, the bacterial genomic DNA was eluted with ethanol and resuspended in 100  $\mu$ L of TE buffer (10 mM Tris-HCl, 1 mM EDTA, pH 8.0). For PCR amplification, a 25  $\mu$ L reaction mixture containing 1  $\mu$ L extracted DNA template, 10 mM 10 $\times$ PCR buffer, 0.2  $\mu$ M forward primer, 0.2  $\mu$ M reverse primer, 0.2 mM dNTPs, 1.75 mM MgCl<sub>2</sub>, and 1 U Taq DNA polymerase was reacted in the PCR device. The amplification conditions were set as follows: pre-denaturation at 95  $^{\circ}$ C for 5 min, 30 cycles of amplification consisting of denaturation at 94  $^{\circ}$ C for 30 s, annealing at 58  $^{\circ}$ C for 30 s, and extension at 72  $^{\circ}$ C for 30 s, and the final extension is at 72  $^{\circ}$ C for 5 min. The primer sequences for *E. coli* O157:H7 [19], *S. aureus* [16], and *L. monocytogenes* [40] were obtained from GENERAL BIOL (Chuzhou, China) and listed in detail in Table S2. PCR amplicons were confirmed by agarose gel electrophoresis.

## Results and discussion

### Investigation of Raman spectra for multiple analysis and Raman enhancement effect

To realize simultaneous multiple detection with SERS, it is the prerequisite to select a group of Raman reporter molecules without inter-spectral interference. The Raman signals of CVa, R6G, MB, Au<sup>CVa</sup>, Au<sup>R6G</sup>, Au<sup>MB</sup>, Au<sup>CVa</sup>@Ag, Au<sup>R6G</sup>@Ag, and Au<sup>MB</sup>@Ag were firstly measured in the suspension dropped onto the glass slide. As measured in Fig. 1A, CVa, R6G, and MB show their distinct characteristic peaks at 586 cm<sup>-1</sup>, 1501 cm<sup>-1</sup>, and 1614 cm<sup>-1</sup>, respectively. Since these Raman reporters have their own characteristic finger spectrum separated from each other at least 100 cm<sup>-1</sup>, it is technically possible to achieve simultaneous multiple detection with these reporters. The inset image gives the structural models of CVa, R6G, and MB, respectively. Secondly, the SERS-Tags should be offered with a strong Raman enhancement effect so that their greatly enhanced Raman signals can benefit for the

improvement of sensitivity. For the verification of SERS effect, results shown in Fig. 1B demonstrate that direct Raman measurement of CVa can just produce the weak signal while a remarkable increase of Raman signal can be observed when CVa is attached on the surface of Au@Ag as the Au<sup>CVa</sup>@Ag. The extraordinary enhancement effect confirms the basis for accurate and sensitive detection of target bacteria. Similarly, the verification results of enhancement effect to the R6G and MB are also demonstrated in Fig. 1C, D, respectively. All these results strongly provide the solid foundation for simultaneous detection of multiple pathogenic bacteria in drink water with the designed strategy.

### Characterization of functional gold nanoparticles and gold nanoparticles @silver nanoparticles

The size and morphology of AuNPs and Au@Ag (exemplified by Au<sup>CVa</sup>@Ag) are characterized by TEM and UV-vis as shown in Fig. 2. Panel a in Fig. 2A shows the example of highly monodispersed spherical AuNPs with average size of 20 nm. After reduced with AgNO<sub>3</sub> on its surface,

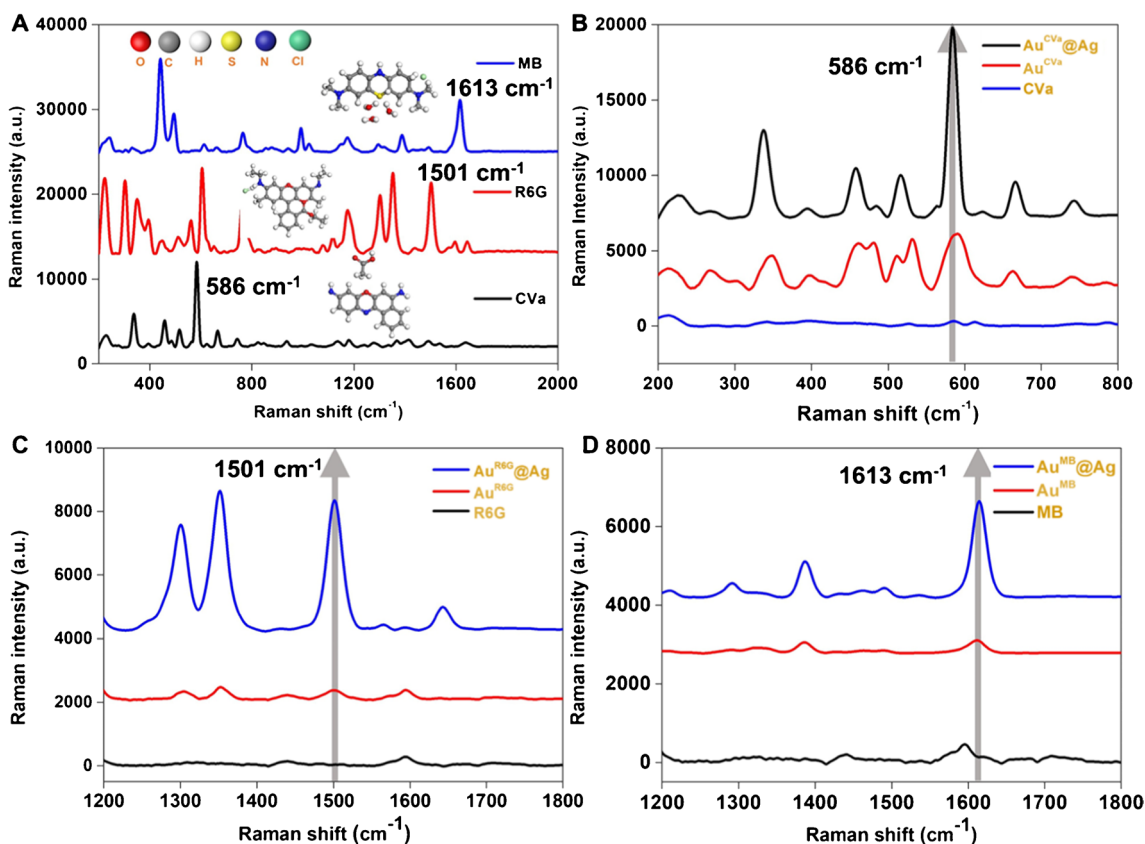
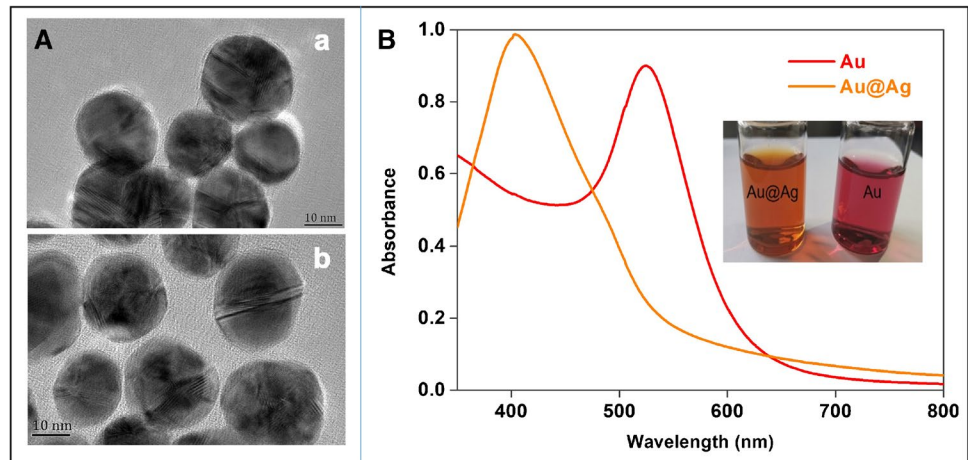


**Fig. 1** A Typical Raman signals of CVa, R6G, and MB with selected characteristic peak at 586 cm<sup>-1</sup> (CVa), 1501 cm<sup>-1</sup> (R6G), 1613 cm<sup>-1</sup> (MB), respectively. Inset gives their structural formulas. **B–D** The

Raman spectra of single Raman reporter, Au<sup>Tag</sup>, and SERS-Tag for CVa, R6G, and MB, respectively. The stepwise intensified Raman intensities show the superior Raman enhancement effect

**Fig. 2** **A** TEM Characterization of AuNPs (a) and Au@Ag (b). **B** UV-vis spectra of AuNPs and Au@Ag. The inset shows photograph of AuNPs and Au@Ag



in panel b of Fig. 2A, it can be clearly observed that the surface of AuNPs is uniformly coated with a layer of silver shell with the thickness of about 2 nm. And the corresponding UV-vis measurements in Fig. 2B exhibits the treatment of AuNPs with  $\text{AgNO}_3$  which led to a distinct blue-shift of peak absorption from 524 nm to 403 nm, indicating the formation of Ag shell. Inset images show the wine-red colored AuNPs changed to orange-yellow colored  $\text{Au}^{\text{CVa}}\text{@Ag}$ . And it is also noted that there is a weak shoulder at ca. 500 nm of the Au@Ag, which could be ascribed to the potential aggregation of the prepared Au@Ag. All these comparison results suggest the successful preparation of functional AuNPs and Au@Ag for SERS measurements. The conjugation of Ab and BSA onto the surface of Au@Ag for recognition and blocking respectively were also characterized with UV-vis. Detailed results in Figure S1 indicate that the modification of Ab and BSA induce the red-shift of 3 nm and 17 nm, respectively, indicating the successful conjugation of Ab and BSA onto the Au@Ag.

### Morphology characterization of the enrichment membrane with SEM

To validate the enrichment ability of the lower enrichment membrane, the morphology of the enrichment membrane is observed before and after utilized for target bacterium enrichment by SEM and demonstrated in Fig. 3. Results in Fig. 3A illustrate the high porosity of the virgin enrichment membrane before utilization. When the water confirmed without bacterium is treated with this enrichment membrane, results in Fig. 3B display the well-shaped pore structure of membrane even though some tiny particles are attached. In contrast, results of filtration of water containing  $1 \times 10^5$  CFU  $\text{mL}^{-1}$  *E. coli* O157:H7 are shown Fig. 3C, demonstrating numerous bacteria entrapped on the surface of the enrichment membrane. To zoom in one collected bacterial cell with TEM, in Fig. 3D, one can see clearly that

many small-sized SERS-Tag<sup>CVa</sup> are tightly and densely distributed on the surface of *E. coli* O157:H7 via antigen-antibody recognition. These morphology characterization results strongly demonstrate the feasibility of this designed two-layer filtration device for effective separation and enrichment of target pathogens on membrane for simultaneous multiple detection. Additionally, the entrapping of *S. aureus* at the concentrations of  $1 \times 10^1$  CFU  $\text{mL}^{-1}$ ,  $1 \times 10^3$  CFU  $\text{mL}^{-1}$ ,  $1 \times 10^5$  CFU  $\text{mL}^{-1}$  on the surface of the enrichment membrane is also characterized by SEM and shown in Figure S2.

### Assay performance investigation on multiple bacteria detection

After feasibility investigation and confirmation, we firstly test the sensing ability of the designed filtration device with only one kind of pathogenic bacterium, respectively. The detailed recorded Raman signals and corresponding linear response against the concentration of target bacterium are depicted in Fig. 4. Typically, in Fig. 4A, for *E. coli* O157:H7 detection, with the increase of *E. coli* O157:H7 concentration in water samples, the number of bacteria collected on the enrichment membrane increases accordingly. And the intensity of the characteristic peak (at  $586 \text{ cm}^{-1}$ ) of CVa is also increased with the increase of amount of *E. coli* O157:H7 in water samples (Fig. 4A). The linear response relationship is also constructed to be  $Y_{\text{CVa}} = 1515.96 \lg X - 21.72$  with a correlation coefficient of 0.9929, in which  $Y_{\text{CVa}}$  and  $X$  stand for the Raman intensity of CVa at  $586 \text{ cm}^{-1}$  and the logarithmic concentration of the target *E. coli* O157:H7, respectively (Fig. 4B). Similarly, the detection results of *S. aureus* and *L. monocytogenes* are also shown in Fig. 4C–F. And the linear responses are  $Y_{\text{R6G}} = 609.99X + 9.94$  ( $R^2 = 0.9854$ ) and  $Y_{\text{MB}} = 981.61X + 79.89$  ( $R^2 = 0.9942$ ), for *S. aureus* and *L. monocytogenes*, respectively. For the detection results of all these target bacteria, the signal of  $1 \times 10^1$  CFU  $\text{mL}^{-1}$  can be well distinguished

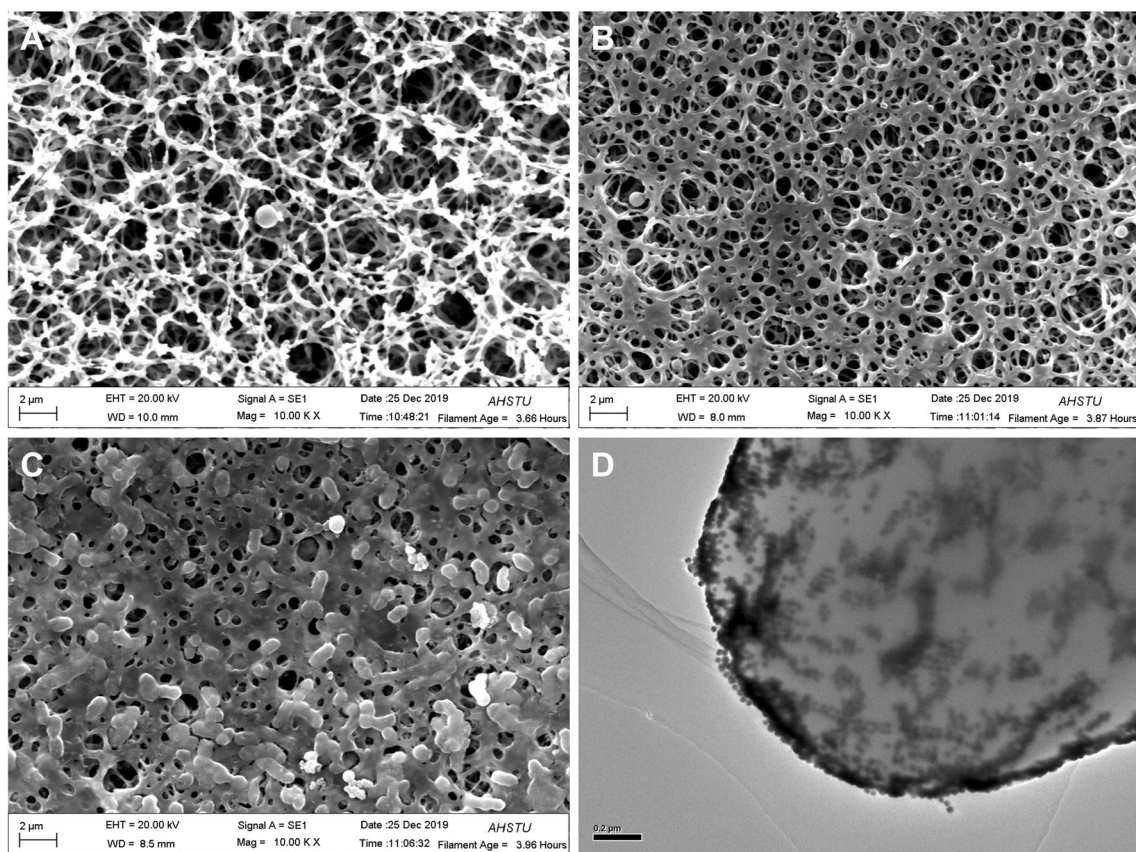


**Fig. 3** SEM images of **A** clean enrichment membrane treated with **B** no bacteria-contaminated lake water and **C** *E. coli* O157:H7 contaminated lake water. **D** TEM image of the surface of one *E. coli* O157:H7 cell to show copious amount of SERS-Tag<sup>Cva</sup> attached

from the blank group, indicating the excellent sensitivity for detection of bacteria in water. This satisfied detection performance can be ascribed to the effective remove of potential interferences with the upper large pore-size membrane and efficient retainment of target bacterium on lower small pore-size membrane for Raman measurement. Comparison results with other reported methods for pathogen detections and also with other SERS methods are described in Table S3. Comparatively, the reported method in this study is much better than others in items of sensitivity, linear range, target species, detection time, and even the detection cost.

Furthermore, any two kinds of the target bacteria are mixed to prepare the spike water samples. Different combinations including the *E. coli* O157:H7/*S. aureus*, *E. coli* O157:H7/*L. monocytogenes*, and *S. aureus*/*L. monocytogenes* are all tested with this designed method, respectively. Detailed SERS results are demonstrated in Fig. 5. Typically, for detection of the combination of *E. coli* O157:H7 and *S. aureus* in the water sample, two characteristic peaks at  $586\text{ cm}^{-1}$  (for *E. coli*O157:H7) of CVa and  $1501\text{ cm}^{-1}$  (for *S. aureus*) of R6G can be observed simultaneously in the Raman results in Fig. 5A. Of note, the intensities of these two peaks show the obvious

concentration-dependent properties of corresponding target bacterium. The recovery rate is calculated according to the constructed linear response relationship in Fig. 4. Detailed recovery results in Table S4 indicate that the quantity of the target bacterium can be well and accurately determined with satisfied recoveries and RSDs in the complicated samples without any interference from other coexisted bacteria. These studies strongly prove the capacity of this designed filtration device for simultaneous determination of multiple bacteria in the same water samples.

Finally, the samples with the mixture of three kinds of bacteria are also evaluated with this designed filtration assisted SERS method. Results in Fig. 6A demonstrate that the corresponding characteristic peak of each target bacterium can be accurately decoded and measured for the quantitative analysis. The recovery studies in Table S5 of each target bacterium are all in the acceptable range. Besides, the collected bacteria in the enrichment membrane are also confirmed with the classical PCR. Results in Fig. 6B also further confirm the accuracy of detection results of our developed method. From all these results, it can come to the conclusion that this designed two membrane-assisted SERS method can be applied for the direct

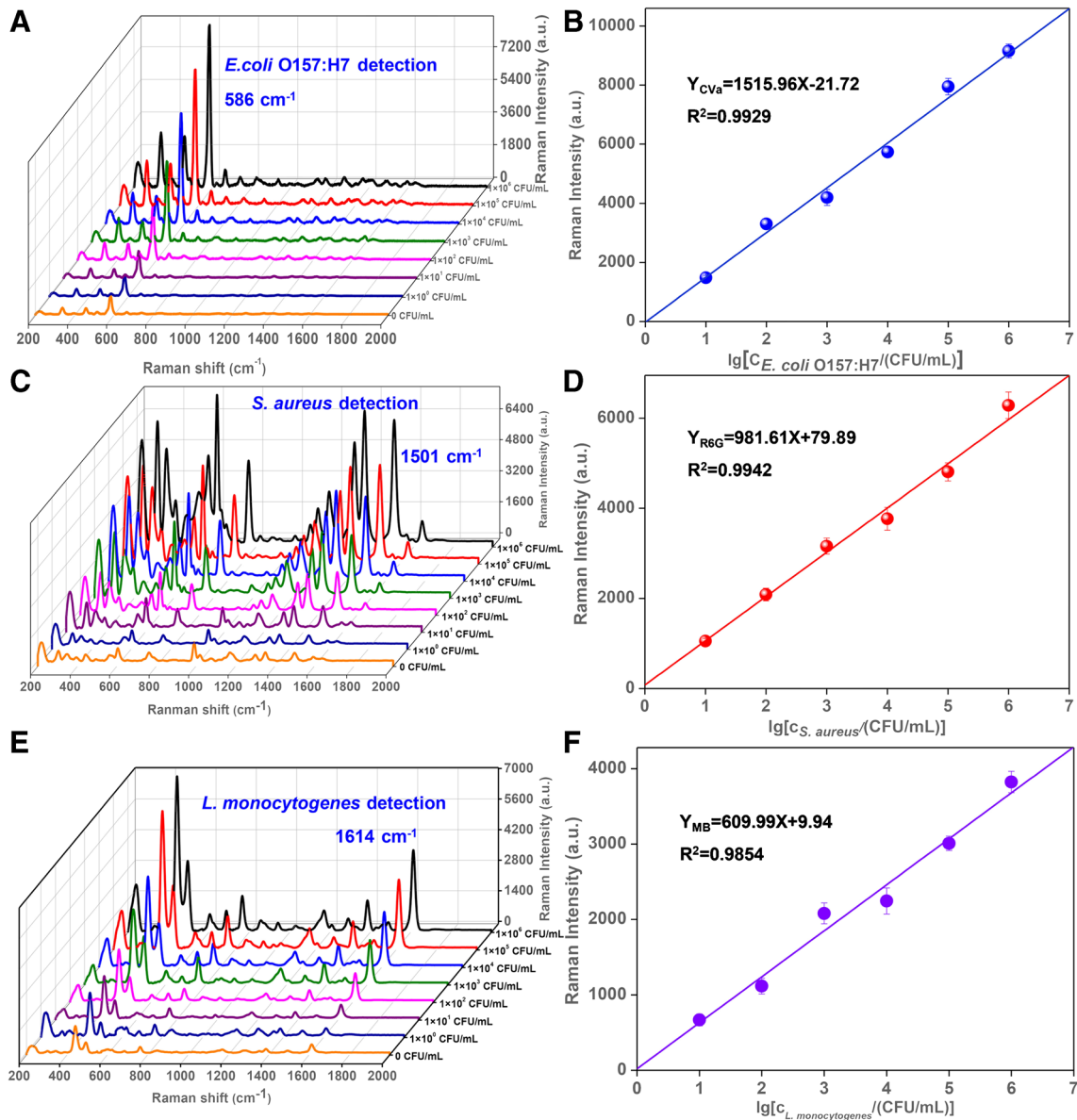


**Fig. 4** Dose–response SERS spectra for *E. coli* O157:H7 (A), *S. aureus* (C), and *L. monocytogenes* (E) detection. The target concentrations from low to high are 0,  $1 \times 10^0$ ,  $1 \times 10^1$ ,  $1 \times 10^2$ ,  $1 \times 10^3$ ,  $1 \times 10^4$ ,  $1 \times 10^5$ , and  $1 \times 10^6$  CFU mL<sup>-1</sup>. Plot of SERS intensity at

peak 586 cm<sup>-1</sup> (B), 1501 cm<sup>-1</sup> (D), and 1614 cm<sup>-1</sup> (F) as a function of logarithm of *E. coli* O157:H7, *S. aureus*, and *L. monocytogenes*, respectively. Error bars are from three independent tests

simultaneous analysis of multiple target bacteria in aqueous samples.

### Specificity evaluation

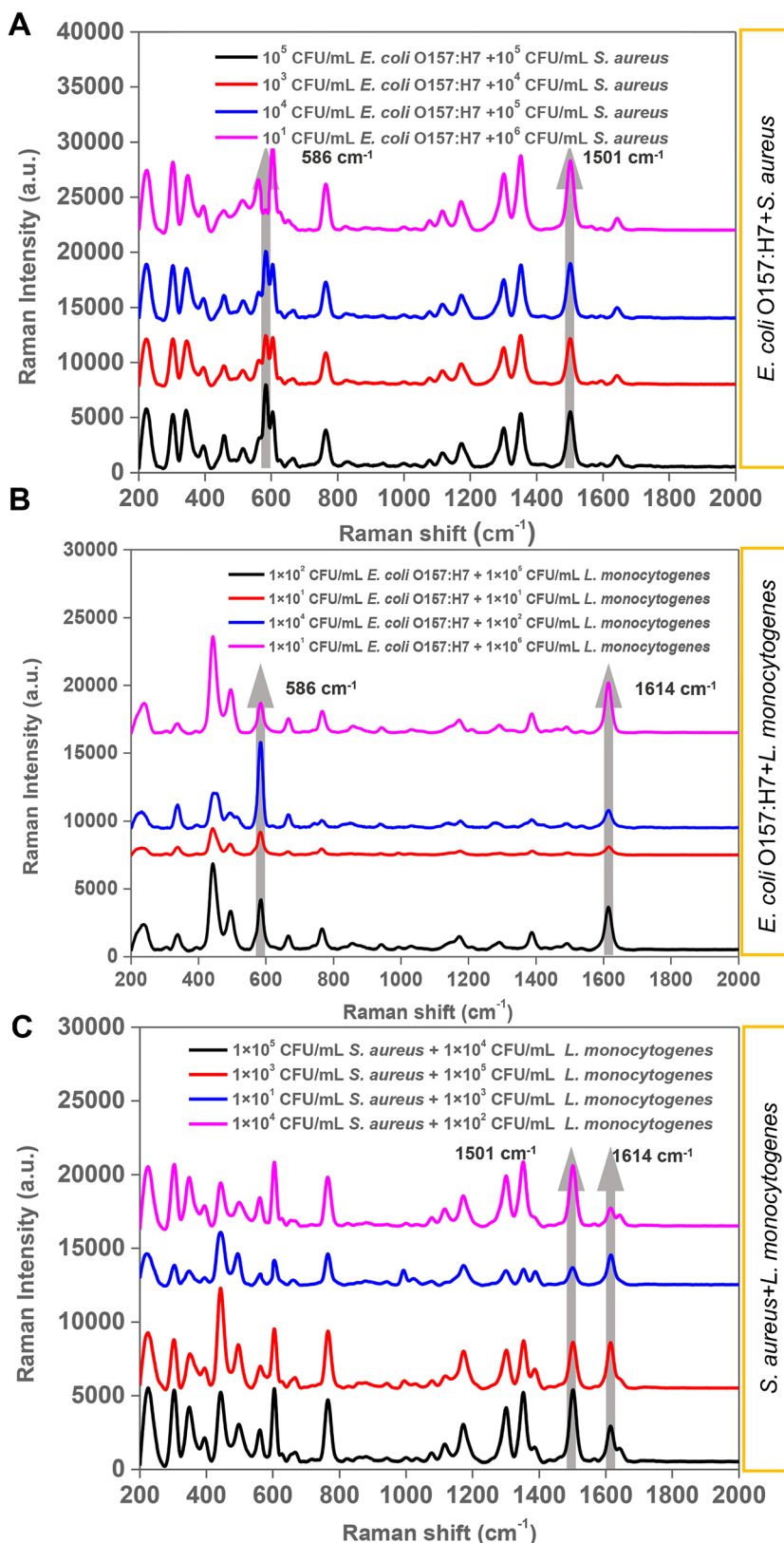
The specificity of our designed filtration-assisted SERS method is also evaluated. As gathered in Fig. 6C, positive Raman signals at their characteristic peaks can only be observed when target *E. coli* O157:H7, *S. aureus*, and *L. monocytogenes* exist. Compared with the Raman intensity results of blank control samples (the right group in Fig. 6C),

the results of other four non-target bacteria including *E. coli*, *P. aeruginosa*, and *S. enteritidis* are also the same as the blank control group, indicating no Raman signal produced of these non-target bacteria.

For the three target bacteria (*E. coli* O157:H7, *S. aureus*, and *L. monocytogenes*), the obvious Raman signals can be easily distinguished from each other compared with both the non-target bacteria and blank control group, indicating an excellent specificity of this device for rapid and multiple bacterial detection and identification. More than that, we also exploited the generality of this device by



**Fig. 5** Representative SERS spectra collected from the target mixtures of *E. coli* O157:H7/*S. aureus* (A), *E. coli* O157:H7/*L. monocytogenes* (B), and *S. aureus*/*L. monocytogenes* (C)



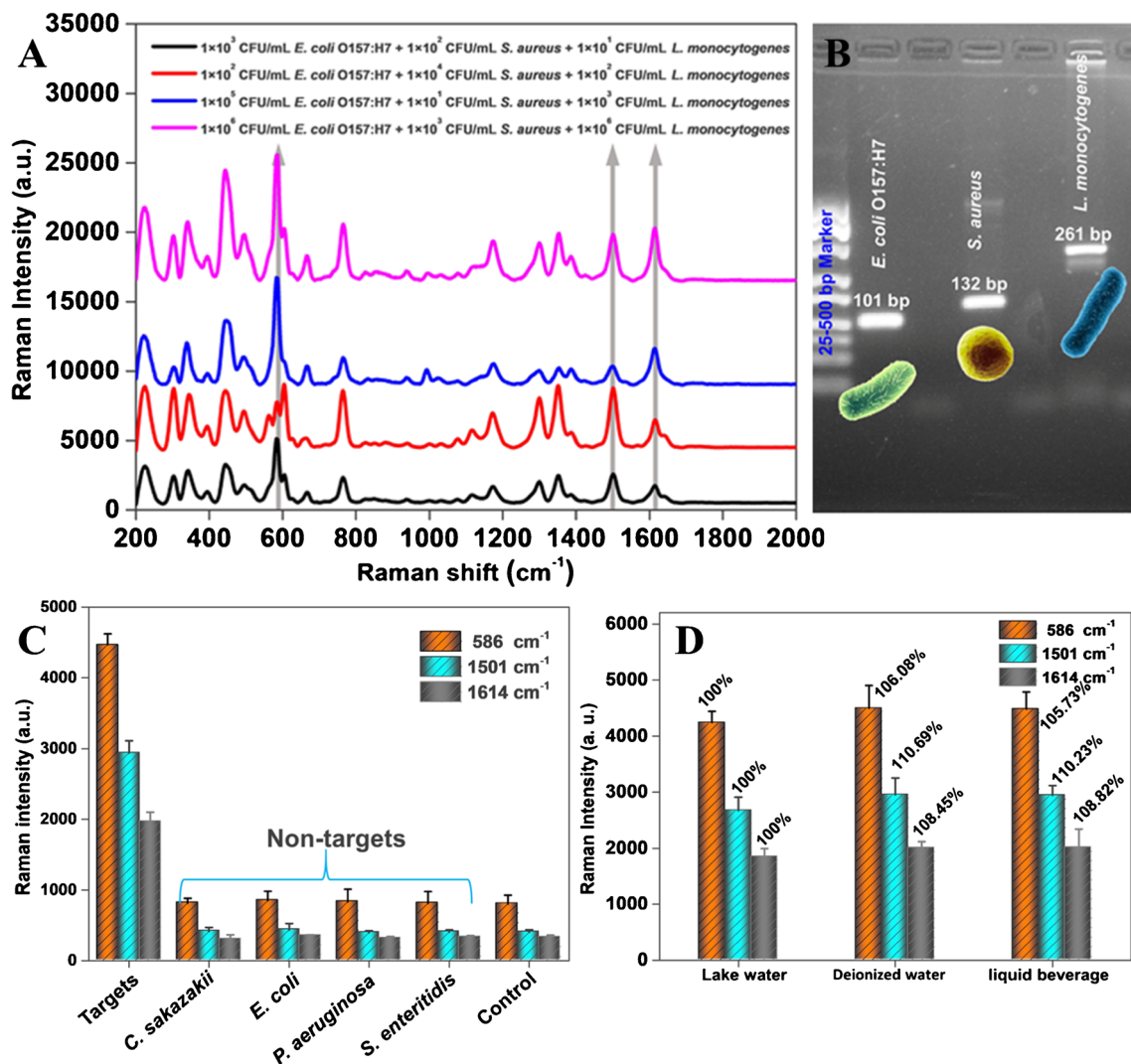


**Fig. 6** **A** Simultaneous SERS decoding of *E. coli* O157:H7, *S. aureus*, and *L. monocytogenes* at different concentrations from lake water. **B** Gel electrophoresis analysis of PCR amplicons from bacteria on the surface of the enrichment membrane. The concentration of each bacterium is  $10^3$  CFU/mL; **C** Raman intensities at characteristic

peaks caused by target bacteria and non-targets. **D** Detection of  $10^3$  CFU/mL *E. coli* O157:H7, *S. aureus*, and *L. monocytogenes* from lake water, deionized water and liquid beverage. Error bars indicate the standard deviations from at least three measurements

comparing the multiple pathogens profiling results of lake water samples with deionized water and liquid beverage samples at the same concentration of various target bacteria. Of note, all aqueous samples have been pre-verified by the classic and gold standard PCR to ensure it did not contain the target bacteria by the Anhui Province Institute of Product Quality Supervision & Inspection. The Raman signal values in lake water are defined as 100% in Fig. 6D. Calculated relative responses of Raman signal in both deionized water and liquid beverage are in great accordance with that achieved in lake water, suggesting the universality and well anti-matrix effect of this designed filtration-assisted SERS method.

## Conclusions

In summary, we have designed and built a portable filtration assisted SERS device for simultaneous detection of multiple target bacteria in water samples. And we have demonstrated its successful use for simultaneous SERS-decoding of three waterborne pathogens. In this study, depending on the design of the device with two membranes with different functions as well as the employment of the SERS-Tags, three kinds of target bacteria are recognized by different SERS-Tag, concentrated onto the enrichment membrane, and measured directly by Raman.

We have demonstrated that this device worked well in lake water with unprecedented detection efficiency, ease of use, and sensitivity. By simple incubation (10 min), injection (10 min), and Raman measurement (5 min) steps, as few as 10 CFU mL<sup>-1</sup> of *E. coli* O157:H7, *S. aureus*, and *L. monocytogenes* can be detected in less than 30 min. The method also shows a broad linear range from 10<sup>1</sup> to 10<sup>6</sup> CFU mL<sup>-1</sup>, an excellent specificity, and functions equally well for aqueous beverages, broadening its wide acceptance. With these characteristics, this straightforward approach offers a new guide for rapid determination of bacteria in identifying infection sources, surveying food chains, and biodefense.

**Supplementary information** The online version contains supplementary material available at <https://doi.org/10.1007/s00604-024-06492-0>.

**Funding** This work was supported by the grants of the grant of Shanghai S&T commission (22N31900500), the Hainan Key Research Program (ZDYF2022XDNY248), the funding of NSFC (32172295), National Key Research Program (2023YFF0611500), and the key R&D program of Anhui (2022k07020009).

**Data availability** Not applicable.

## Declarations

**Ethical approval** Not applicable.

**Conflict of interest** The authors declare no competing interests.

## References

- Kazi M, Annapure US (2016) Bacteriophage biocontrol of food-borne pathogens. *J Food Sci Tech* 53:1355–1362
- Sharma H, Mutharasan R (2013) Review of biosensors for food-borne pathogens and toxins. *Sens Actuat B-Chem* 183:535–549
- Shaw A, Helterbran K, Evans MR (2016) Currey growth of *Escherichia coli* O157:H7, non-O157 Shiga toxin-producing *Escherichia coli*, and *Salmonella* in water and hydroponic fertilizer solutions. *J Food Protect* 79:2179–2183
- Armstrong RW, Fung PC (1993) Brainstem encephalitis (rhombencephalitis) due to *Listeria monocytogenes*: case report and review. *Clin Infect Dis* 16:689–702
- Besser RE, Griffin PM, Slutsker L (1999) *Escherichia coli* O157:H7 gastroenteritis and the hemolytic uremic syndrome: an emerging infectious disease. *Annu Rev Med* 50:355–367
- Goss CH, Muhlebach MS (2011) Review: *Staphylococcus aureus* and MRSA in cystic fibrosis. *J Cyst Fibros* 10:298–306
- Griffin PM, Tauxe RV (1991) The epidemiology of infections caused by *Escherichia coli* O157:H7, other enterohemorrhagic *E. coli*, and the associated hemolytic uremic syndrome. *Epidemiol Rev* 13:60–98
- Varma PRG, Cochin TSG (2013) Viability of *Listeria monocytogenes* in water. *Fish Technol* 30:164–165
- Wang G, Doyle MP (1998) Survival of enterohemorrhagic *Escherichia coli* O157:H7 in water. *J Food Prot* 61:662–667
- Bai N, Sun P, Zhou H, Wu H, Wang R, Liu F, Zhu W, Lopez JL, Zhang J, Fang J (2011) Inactivation of *Staphylococcus aureus* in water by a cold, He/O<sub>2</sub> atmospheric pressure plasma microjet. *Plasma Process Polym* 8:424–432
- Chen CY, Wu LC, Chien CY (2010) Inactivation of *Staphylococcus aureus* and *Escherichia coli* in water using photocatalysis with fixed TiO<sub>2</sub>. *Water Air Soil Poll* 212:231–238
- Nwachuku N, Gerba CP (2008) Occurrence and persistence of *Escherichia coli* O157:H7 in water. *Rev Environ Biotechnol* 7:267–273
- Stea EC, Purdue LM, Jamieson RC, Yost CK, Truelstrup Hansen L, Bjrkroth J (2015) Comparison of the prevalences and diversities of *Listeria* species and *Listeria monocytogenes* in an urban and a rural agricultural watershed. *Appl Environ Microbiol* 81:3812
- Poullis DA, Attwell RW, Powell SC (2005) The characterization of waterborne-disease outbreaks. *Rev Environ Health* 20:141–149
- Magdalena B, Rita S, Weintraub JM (2006) Review of syndromic surveillance: implications for waterborne disease detection. *J Epidemiol Commun H* 60:543–550
- Mehrotra M, Wang GH, Johnson WM (2000) Multiplex PCR for detection of genes for *Staphylococcus aureus* enterotoxins, exfoliative toxins, toxic shock syndrome toxin 1, and methicillin resistance. *J Clin Microbiol* 38:1032–1035
- Qin P, Xu J, Yao L, Wu Q, Chen W (2020) Simultaneous and accurate visual identification of chicken, duck and pork components with the molecular amplification integrated lateral flow strip. *Food Chem* 339:127891
- Yeon JJ, Kyu YH, An S, Won LJ, Eu-Ree A, Yeon-Ji K, Hyun-Chul P, Kyungmyung L, Ho HJ, Si-Keun L (2018) Rapid oral bacteria detection based on real-time PCR for the forensic identification of saliva. *Sci Rep* 8:10852
- Spano G, Beneduce L, Terzi V, Stanca AM, Massa S (2010) Real-time PCR for the detection of *Escherichia coli* O157:H7 in dairy and cattle wastewater. *Lett Appl Microbiol* 40:164–171
- Safavieh M, Ahmed MU, Ng A, Zourob M (2014) High-throughput real-time electrochemical monitoring of LAMP for pathogenic bacteria detection. *Biosens Bioelectron* 58:101–106
- Azizi M, Zaferani M, Cheong SH, Abbaspourrad A (2019) Pathogenic bacteria detection using RNA-based loop-mediated isothermal-amplification-assisted nucleic acid amplification via droplet microfluidics. *ACS Sens* 4:841–848
- Huang TT, Liu SC, Huang CH, Lin CJ, Huang ST (2018) An integrated real time electrochemical LAMP device for pathogenic bacteria detection in food. *Electroanal* 30:2397–2404
- Lutz S, Weber P, Focke M, Faltin B, Hoffmann J, Müller C, Mark D, Roth G, Munday P, Armes N (2010) Microfluidic lab-on-a-foil for nucleic acid analysis based on isothermal recombinase polymerase amplification (RPA). *Lab Chip* 10:887–893
- Moll N, Pascal E, Dinh DH, Pillot JP, Bennetau B, Rebière D, Moynet D, Yan M, Mossalayi D, Pistré J (2007) A love wave immunosensor for whole *E. coli* bacteria detection using an innovative two steps immobilisation approach. *Biosens Bioelectron* 22:2145–2150
- Sun X, Sharma S, Lee G, Park S, Kim M (2016) Detection of *Cronobacter* genus in powdered infant formula by enzyme-linked immunosorbent assay using anti-*Cronobacter* antibody. *Front Microbiol* 7:1124
- Fernández D, Rodríguez EM, Arroyo GH, Padola NL, Parma AE (2010) Seasonal variation of Shiga toxin-encoding genes (stx) and detection of *E. coli* O157 in dairy cattle from Argentina. *J Appl Microbiol* 106:1260–1267
- Akesson M, Karlsson EN, Hagander P, Axelsson JP, Tocaj A (1999) On-line detection of acetate formation in *Escherichia coli* cultures using dissolved oxygen responses to feed transients. *Biotechnol Bioeng* 64:590–598
- Thacker VV, Herrmann LO, Sigle DO, Zhang T, Liedl T, Baumberg JJ, Keyser UF (2014) DNA origami based assembly of gold

- nanoparticle dimers for surface-enhanced Raman scattering. *Nat Commun* 5:3448
29. Rycenga M, Wang Z, Gordon E, Cobley CM, Xia Y (2010) Probing the photothermal effect of gold-based nanocages with surface-enhanced Raman scattering (SERS). *Angew Chem Int Ed* 48:9924–9927
  30. Graham D, Duyn RV, Ren B (2016) Surface-enhanced Raman scattering. Springer
  31. Yang X, Gu C, Qian F, Jin L (2011) Highly sensitive detection of proteins and bacteria in aqueous solution using surface-enhanced Raman scattering and optical fibers. *Anal Chem* 83:5888–5894
  32. Liu Y, Zhou H, Hu Z, Yu G, Yang D, Zhao J (2017) Label and label-free based surface-enhanced Raman scattering for pathogen bacteria detection: a review. *Biosens Bioelectron* 94:131–140
  33. Wang J, Wu X, Wang C, Rong Z, Ding H, Li H, Li S, Shao N, Dong P, Xiao R (2016) Facile synthesis of Au-coated magnetic nanoparticles and their application in bacteria detection via a SERS method. *ACS Appl Mater Inter* 8:19958–19967
  34. Rodden G (2015) The drinkable book. Pulp & Paper International
  35. Tokonami S, Nakadoi Y, Takahashi M, Ikemizu M, Kadoma T, Saimatsu K, Dung LQ, Shiigi H, Nagaoka T (2013) Label-free and selective bacteria detection using a film with transferred bacterial configuration. *Anal Chem* 85:4925–4929
  36. Talley CE, Jackson JB, Oubre C, Grady NK, Hollars CW, Lane SM, Huser TR, Nordlander P, Halas NJ (2005) Surface-enhanced Raman scattering from individual Au nanoparticles and nanoparticle dimer substrates. *Nano Lett* 5:1569–1574
  37. Zhang X, Su Z (2012) Polyelectrolyte-multilayer-supported Au@Ag core-shell nanoparticles with high catalytic activity. *Adv Mater* 24:4574–4577
  38. Xing S, Feng Y, Tay YY, Chen T, Xu J, Pan M, He J, Hng HH, Yan Q, Chen H (2010) Reducing the symmetry of bimetallic Au@Ag nanoparticles by exploiting eccentric polymer shells. *J Am Chem Soc* 132:9537–9539
  39. Johnson G, Nour AA, Nolan T, Huggett J, Bustin S (2014) Minimum information necessary for quantitative real-time PCR experiments. *Methods Mol Biol* 1160:5–17
  40. Rawool DB, Doijad SP, Poharkar KV, Negi M, Kale SB, Malik SVS, Kurkure NV, Chakraborty T, Barbuddhe SB (2016) A multiplex PCR for detection of *Listeria monocytogenes* and its lineages. *J Microbiol Meth* 130:144–147

**Publisher's note** Springer Nature remains neutral with regard to jurisdictional claims in published maps and institutional affiliations.

Springer Nature or its licensor (e.g. a society or other partner) holds exclusive rights to this article under a publishing agreement with the author(s) or other rightsholder(s); author self-archiving of the accepted manuscript version of this article is solely governed by the terms of such publishing agreement and applicable law.